

Selective Crystallization of Four Bis(phthalocyaninato)neodymium(III) Polymorphs

*Maegan Dailey, Claire Besson**

Department of Chemistry, The George Washington University, 800 22nd Street NW,
Washington, D.C. 20052, United States

ABSTRACT: Four polymorphs of bis(phthalocyaninato)neodymium(III) were reproducibly and selectively crystallized by the slow evaporation of saturated solutions. The obtained phase depended on the initial oxidation state of the NdPc₂ molecule and the choice of solvent. Single-crystal X-ray diffraction studies were used to correct previous mis-identifications and provide missing coordinates for the γ -phase as well as a detailed comparison of molecular structure and crystal packing in all NdPc₂ polymorphs. The primary feature in all phases is columnar stacking based on parallel π - π interactions, with a variety of slip angles within those stacks as well as secondary interactions between them. Chemical redox and acid-base titrations, performed on re-dissolved crystals demonstrate that NdPc₂⁺ and NdPc₂⁻ are easily obtained through weak oxidizing and reducing agents, respectively. Additionally, we show that the protonated form of the NdPc₂⁻ complex has a nearly identical UV-Vis spectra to that of neutral NdPc₂, explaining some of the confusion over chemical composition in previously published literature.

INTRODUCTION

Bis(phthalocyaninato)lanthanoid (LnPc_2) compounds were first reported by Kirin and Moskalev in the mid-1960s.¹ In these compounds, a trivalent lanthanoid ion is sandwiched between two macrocyclic phthalocyanine (Pc) ligands, with the four isoindole nitrogen atoms of each Pc coordinating to the lanthanoid. The resulting double-decker complexes generally have a square antiprism coordination sphere. Since the 1960s, these species have been intensely studied due to their unique properties, including electrochromism², semiconductivity³, photoconductivity³, and high chemical and thermal stabilities⁴, which arise from the intramolecular π - π interactions of the Pc ligands and the presence of $4f$ orbitals on the metal center.⁵ Because of these properties, diphthalocyanine complexes have been integrated in solar cells⁶ and field effect transistors⁷, and studied as molecular magnets⁸ and information storage materials.⁹

Modifications of Kirin and Moskalev's original synthesis resulted in double-decker compounds across the lanthanoid series¹⁰⁻²⁵ (with the exception of radioactive promethium), as well as for several actinoid²⁶⁻³¹, p-block³²⁻³⁵, and transition metals.³⁶ Crystals of varying quality used in structure determinations were grown through electrochemical methods, solvent-solvent diffusion, and sublimation. Several polymorphs and a dichloromethane solvate phase have been identified for homoleptic, unsubstituted double-decker compounds (**Table 1**). The γ -phase, densest of the non-solvated phases, is the most commonly observed.

Table 1. Reported MPC₂ Polymorphs

Phase	α -phase	β -phase	γ -phase	δ -phase	CH ₂ Cl ₂ solvate phase	N/A
Space Group	$P4/nnc$	$C2/c$	$P2_12_12_1$	$C2/c$	$Pnma$	$P\bar{1}$
Unit Cell Parameters	$a = b = 19.9 \text{ \AA}$ $c = 6.4 \text{ \AA}$ $\alpha = \beta = \gamma = 90^\circ$ ^a	$a = 19.0 \text{ \AA}$ $b = 19.1 \text{ \AA}$ $c = 15.5 \text{ \AA}$ $\alpha = \gamma = 90^\circ$ $\beta = 116.1^\circ$ ^a	$a = 8.8 \text{ \AA}$ $b = 10.6 \text{ \AA}$ $c = 50.8 \text{ \AA}$ $\alpha = \beta = \gamma = 90^\circ$ ^a	$a = 28.1 \text{ \AA}$ $b = 14.2 \text{ \AA}$ $c = 13.2 \text{ \AA}$ $\alpha = \gamma = 90^\circ$ $\beta = 115.6^\circ$ ^a	$a = 28.1 \text{ \AA}$ $b = 22.9 \text{ \AA}$ $c = 7.9 \text{ \AA}$ $\alpha = \beta = \gamma = 90^\circ$ ^a	$a = 13.4 \text{ \AA}$ $b = 13.4 \text{ \AA}$ $c = 16.3 \text{ \AA}$ $\alpha = 68.7^\circ$ $\beta = 65.9^\circ$ $\gamma = 74.7^\circ$
Metal Center	Pr, ^{b,13} Nd, ^{b,15,17,18} Er, ^{b,23} Eu, ^{c,31} Am ^{c,31}	Sn, ³³ Ce, ^{b,24} Nd, ^{b,16} Th, ^{27,29} Pa, ³⁰ U ^{26,29}	Y, ^{19,21} In, ³² Sn ³³ Nd, ^{b,17} Gd ¹⁰ , Tb ^{19,22} , Dy ^{19,22} , Lu ¹¹	Pr, ^{b,d,12} Nd ^{c,18}	Y ²¹ , In ²¹ , La ^{b,25} Bi ^{b,35} , Nd ¹⁴ , Tb ²¹ , Lu ¹⁰	Zr ³⁶

^a Unit cell parameters of the neodymium complex. ^b Crystals grown by electrochemical methods.

^c Crystallization method unknown. ^d Authors used non standard $I2/c$ space group.

Bis(phthalocyaninato)neodymium (III) is unique among the double-deckers in forming the α -^{13,17,18}, β -¹⁶, γ -¹⁸, δ -¹⁸, and CH₂Cl₂ solvate polymorphs^{14,15}. The crystal structures were first reported in the 1980s, using crystals grown through electrochemical oxidation of the anionic NdPc₂⁻ complex, with the exception of the CH₂Cl₂ solvate phase, which was obtained by the re-crystallization of a powder from CH₂Cl₂.¹³⁻¹⁸ These methods often resulted in small, low quality crystals or powders that led to mis-identified space groups and/or phase identification that was only possible by comparison with another complex, with no coordinate determination. Though single crystals of functionalized double- and triple-decker (Ln₂Pc₃) complexes have been obtained through solvent-solvent diffusion, there has been limited success with synthesizing

NdPc₂ in large yields and in growing crystals suitable for X-ray diffraction studies without electrochemical methods.³⁷⁻⁴⁰ This has limited the ability to study the structures of the various polymorphs and their impact on other properties.

Additionally, there has been confusion in the previously published literature about the exact chemical composition of the NdPc₂ species.^{14,15} Bis(phthalocyaninato)lanthanoid complexes can easily undergo oxidation and reduction reactions to give the charged complexes LnPc₂⁺ and LnPc₂⁻, respectively. The neutral and negatively charged species are deep green or purplish blue, while the cation is red, making them perfect candidates for identification by UV-Vis spectroscopy. However, some of the species, e.g. LnPc₂ and HLnPc₂, can have very similar spectra, and care should be taken in relying solely on UV-Vis spectra for identification.

Here, we report the straightforward, reproducible and selective crystallization of four of the five known NdPc₂ polymorphs, without the use of electrochemical methods. An investigation of these polymorphs, conducted by single-crystal X-ray diffraction, allows for a detailed structural comparison between all five polymorphs. Additionally, through chemical titrations, we provide the definitive spectra of charged complexes NdPc₂⁺ and NdPc₂⁻ as well as protonated HNdpC₂.

EXPERIMENTAL SECTION

Materials and Methods

Neodymium (III) acetate hydrate (Alfa Aesar) and phthalonitrile (TCI) were used as received. Hexanol (ACROS) was dried over Grade 562 3 Å molecular sieves (Fisher) and stored under nitrogen. Lithium methoxide was prepared by reacting solid lithium metal (Merck) with an excess of dry, degassed methanol (Fisher).

Synthesis

All NdPc₂ complexes were synthesized according to previously published procedures with some modifications.¹⁰ Phthalonitrile (200 mg, 1.6 mmol), neodymium (III) acetate hydrate (50 mg, 0.15 mmol), and lithium methoxide (200 mg, 5.3 mmol) were added to a round bottom flask and placed under a protective nitrogen atmosphere. Dry hexanol (10 mL) was then added to the flask, and the temperature was increased to 160°C. The mixture was left to reflux for 18.5 hours, after which it was allowed to cool to room temperature. The hexanol was removed under reduced pressure at 65°C, leaving a blue-green solid. The solid was dissolved in a minimum amount of acetone via sonication, adsorbed onto silica gel, and purified by column chromatography using a CH₂Cl₂/EtOH gradient as eluent. Pure CH₂Cl₂ eluted one dark blue band containing the NdPc₂⁻ complex. The volume of EtOH was slowly increased to a maximum ratio of 70:30 v:v CH₂Cl₂:EtOH to remove the remaining blue-green and green bands. The green band eluted as one long band that appeared to contain several different shades of green (see Supplementary Information), due to different levels of purity. UV-Vis analysis of the fractions indicated that the blue-green fractions were a mixture of anionic and neutral phases, while green-yellow fractions were the co-elution of neutral NdPc₂ and oligomeric phthalonitrile formed during the reaction. Dark and light green fractions were neutral NdPc₂ with no impurities. Fractions were characterized by UV-Vis spectroscopy after purification was completed. Single crystals for all phases were grown by slow evaporation from a concentrated solution, in air, at room temperature. A solution of neutral NdPc₂ in 98:2 v:v CHCl₃:EtOH resulted in small (0.4 mm), dark green rectangular plates, determined to be the α-phase, while pure CHCl₃ produced dark green blocks shown to be the γ-phase. The δ-phase was produced from a solution of anionic NdPc₂⁻ in either 98:2 v:v CHCl₃:EtOH or pure CHCl₃ as large (1.2 mm), dark green rectangular

plates. Slow evaporation of a CH₂Cl₂ solution containing neutral NdPc₂ or reduced NdPc₂⁻ resulted in the CH₂Cl₂ solvate phase as green needles of various sizes.

X-Ray Structure Determination

Single crystals were isolated from the bulk samples and mounted on MiTeGen micromounts.

Reflection data was collected at 100(2) K with 0.5° ω scans on a Bruker SMART diffractometer with an APEX II CCD detector using Mo K α (λ = 0.71073 Å) radiation. The data was integrated using the SAINT⁴¹ program within the APEX II⁴² software suite. An absorption correction was applied using SADABS.⁴³ All structures were solved with direct methods using SIR 92⁴⁴ and refined with SHELXL 2018/3.⁴⁵ The WinGX⁴⁶ software suite was used to refine the γ -, δ - and CH₂Cl₂ solvate phases while ShelXle⁴⁷ was used to refine the α -phase. For every structure, all non-hydrogen atoms were located in difference Fourier maps and refined anisotropically.

Aromatic hydrogen atoms, while located in the difference Fourier maps, were placed in position with the HFIX43 command. The hydrogen atoms in the dichloromethane molecule were placed in position with the HFIX23 command. Platon⁴⁸ was used to check all structures for additional symmetry while Mercury⁴⁹ was used to visualize structures, generate thermal ellipsoid plots, and create figures. Thermal ellipsoid plots for all phases can be found in the Supporting Information.

Spectroscopic Characterization

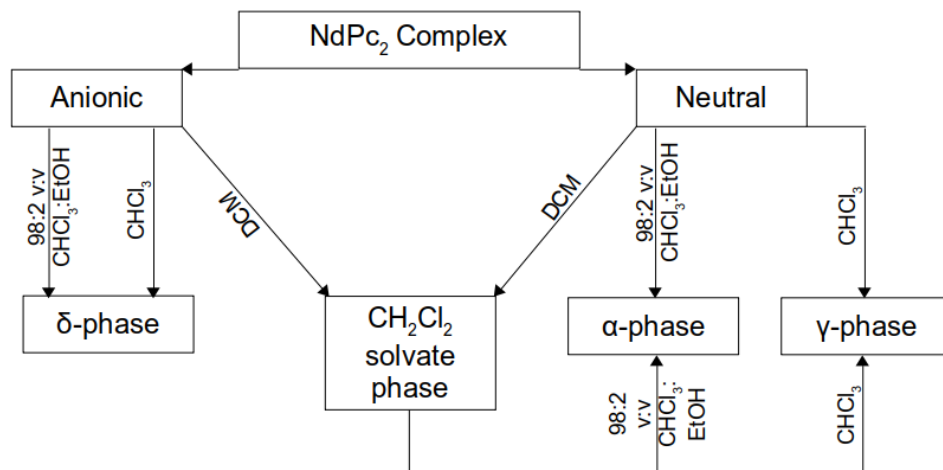
Solution UV-Vis spectra were recorded on an Analytik Jena Specord 1500 UV-Vis spectrophotometer. A few drops of concentrated chromatography fractions were placed in a quartz cuvette and diluted with CH₂Cl₂ to a concentration of approx. 2.5×10^{-7} M. For chemical redox titrations, several milligrams of single crystals were isolated from the bulk sample, placed in a quartz cuvette, and dissolved in CH₂Cl₂. Solutions of iodine (I₂, 0.05 M) and triethylamine

(NEt₃, 0.05 M) in CH₂Cl₂ were added in microliter increments and UV-Vis spectra were recorded after each addition. This process was repeated, under nitrogen, for acid-base titrations, using concentrated glacial acetic acid, concentrated 1,8-diazabicyclo[5.4.0]undec-7-ene (DBU) and a solution of re-dissolved γ -phase crystals.

RESULTS AND DISCUSSION

Bis(phthalocyaninato)neodymium (III) is synthesized from phthalonitrile and neodymium acetate in refluxing hexanol using a 10:1 ratio of phthalonitrile to neodymium. This ratio limits the amount of metal-free phthalocyanine, single- and triple-decker complexes produced in the reaction. Purification by chromatography gives neutral NdPc₂ and anionic NdPc₂⁻, the latter of which slowly re-oxidizes to give the former in solutions exposed to air. Crystallization by slow evaporation gives analytically pure NdPc₂, though the conditions of crystallization results in four different polymorphs (Scheme 1): the α -, γ -, δ - and CH₂Cl₂ solvate phases.

Scheme 1. Crystallization conditions for NdPc₂ polymorphs.



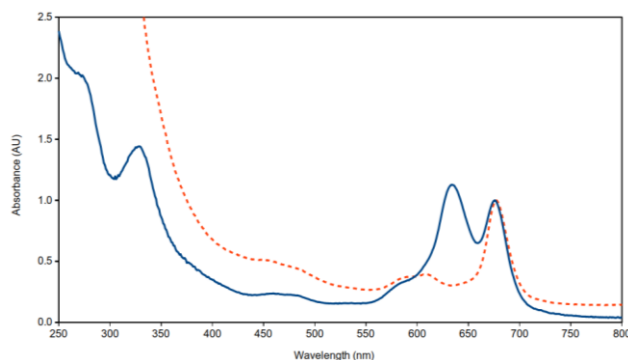


Figure 1. Normalized UV-Vis spectra of the mother liquor of the δ -phase (blue) and crystals freshly dissolved in CH_2Cl_2 (red dashes).

The δ -phase is exclusively obtained from mother solutions containing NdPc_2^- , which O_2 oxidizes in situ to NdPc_2 . The anion, however, is not substantially incorporated in the resulting crystal structure, as demonstrated by the UV-Vis spectrum of dissolved crystals (Figure 1). The spectrum is characteristic of neutral NdPc_2 molecules, with three main peaks: a Q band at 678 nm, resulting from a π - π^* HOMO-LUMO transition, a broad intervalence band covering the 450-500 nm range, due to the delocalization of a radical electron across both Pc ligands, and a B (or Soret) band around 320 nm corresponding from an additional π - π^* transition.^{50,51} By contrast, the mother liquor of the δ -phase shows a more intense B band and a split Q band, with one component blue-shifted to 638 nm, characteristic of reduced NdPc_2^- .

While the initial oxidation state of the sandwich complex is determinant in the formation of the δ -phase, the choice of solvent is crucial for polymorph selectivity when starting from neutral NdPc_2 (Scheme 1): solutions in pure chloroform provide the γ -phase while 98:2 v:v mixtures of chloroform and ethanol yield the α -phase. Dichloromethane, whenever present, is incorporated in the solid to form the $\text{NdPc}_2 \cdot \text{CH}_2\text{Cl}_2$ solvate phase. Interconversion between polymorphs is readily accomplished by dissolving crystals in the appropriate solvent and allowing the saturated solution to slowly evaporate.

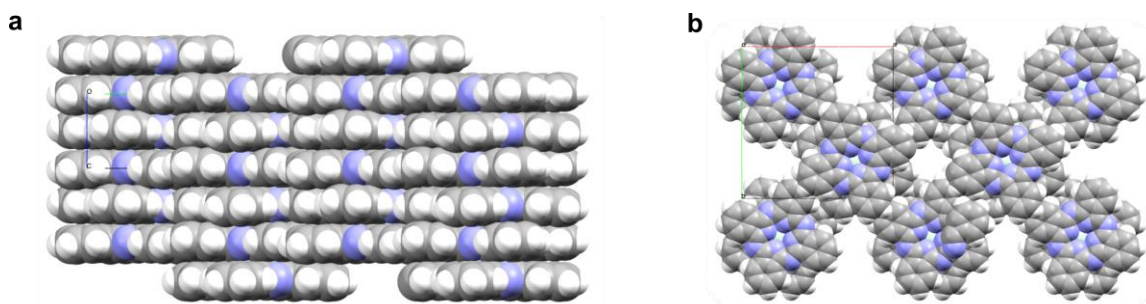


Figure 2. Space-filling model of the structure of the α -phase, viewed along the [100] (a) and the [001] directions (b). Color code: Nd, light green; N, blue; C, grey; H, white.

The α -phase, consistently obtained by slow evaporation of a 98:2 v:v CHCl_3 :EtOH, presents as continuous columns of NdPc_2 molecules arranged in a square lattice reminiscent of the typical arrangement observed for LnPc_2 mono- and bilayers on metallic surfaces,^{19,53-62} but with every second stack displaced vertically by a Pc-Pc distance (**Figure 2**). The asymmetric unit contains 1/8th of the NdPc_2 molecule. The remainder of the D_4 -symmetry complex is generated by a 4-fold axis and perpendicular 2-fold axes through the Nd^{3+} center. The Nd-N distance is 2.476(5) Å, a value that remains constant across all polymorphs. The Nd^{3+} ion has an approximately square antiprism coordination geometry with a skew angle (**Figure 3**) of 40.9° between the two slightly curved Pc rings. Molecules within the columns interact via cofacial π - π stacking⁵² (slip angle $\varphi = 90^\circ$, twist angle $\psi = 0$, Nd-Nd distance 6.4202(16) Å), while stacks are separated by weak H \cdots H contacts at a distance of 2.3077(5) Å. Additionally, a 87:13 disorder is observed between two neodymium positions related by a vertical shift of the NdPc_2 column by the length of one Pc-Pc spacing.

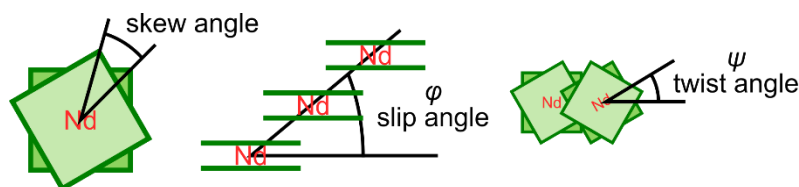


Figure 3. Definition of the skew, slip and twist angles with phthalocyanine rings schematized as squares.

This disorder combined with the high symmetry of the packing have contributed in the past to a number of errors in both space group and structure determination.^{13,17,63} Mossoyan-Deneux *et al.* assigned the minor neodymium contribution as a fractional oxide or chloride anion,⁶³ a hypothesis which can easily be dismissed based on the UV-visible spectra of the freshly dissolved crystals showing no NdPc_2^+ signal. Darovsky *et al.* observed a 72:28 disorder between the two neodymium positions, which they modeled by a $3 \times 3 \times 1$ supercell of columns alternatively shifted by $c/2$, accounting for a 75:25 disorder ratio, with the additional disorder due to the presence of small amounts of the triple decker complex Nd_2Pc_3 . However, we found no evidence of a super-cell or super-structure in our diffraction data (Figure S4), in agreement with our significantly lower disorder ratio. Nd_2Pc_3 was not detected in our UV-visible investigations, nor was it present in samples of the α -phase obtained by recrystallization of another polymorph. Given the weakness of the inter-column interactions (weak $\text{H} \cdots \text{H}$ contacts, no interlocking molecules), and the resulting low enthalpy cost of the shift of a NdPc_2 column across the whole crystal, we hypothesize that the observed disorder is exclusively due to random surface alignment defects propagated throughout the growth of the crystal.

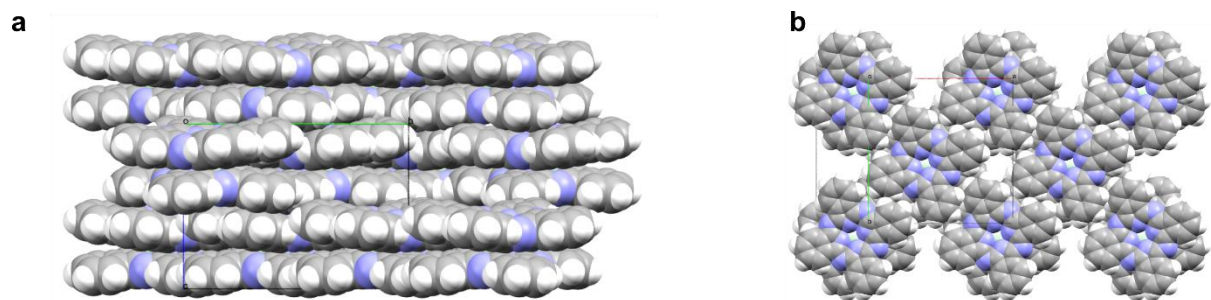


Figure 4. Space-filling model of (a) the structure of the β -phase, viewed along the $[100]$ direction and (b) the monolayer of complexes formed in the (110) plane. Color code: Nd, light green; N, blue; C, grey; H, white. Hydrogen atoms have been added to the published structure to facilitate comparison between the polymorphs.

The β -phase was previously grown by electrochemical methods¹⁶ and could not be reproduced by either slow evaporation or solvent-solvent diffusion in this work. We will give here, for completion, a brief description of the structure as reported by Darovskikh et al.¹⁶ The C_2 -symmetry $NdPc_2$ molecule is generated from the asymmetric unit (one Pc ring and half the Nd center) by a 2-fold axis that runs parallel to the Pc ring and through the Nd^{3+} center. The resulting molecule has a square antiprism geometry with Nd-N distances of 2.46-2.48 Å and a skew angle of $39.0^\circ(\pm 1.2)$. Compared to the α -phase, the Pc ligands in this phase have a much more pronounced saucer-shape. The double-decker complexes are assembled via π - π parallel-displaced slipped stacking²⁰ in stacks progressing in zig-zag along the $[100]$ direction (**Figure 4a**). The slip angle within the stack is $\varphi = 49.5^\circ$, corresponding to a Nd-Nd distance of 8.458 Å. The molecule-to-molecule twist angle of $\psi = -39^\circ$ is opposite to the skew angle, yielding a parallel alignment of the Pc rings facing each other. The stacks are arranged, via $H\cdots H$ contacts at 2.111 and 2.265 Å, in a square lattice almost identical to that of the α phase, but here without any vertical displacement (**Figure 4b**).

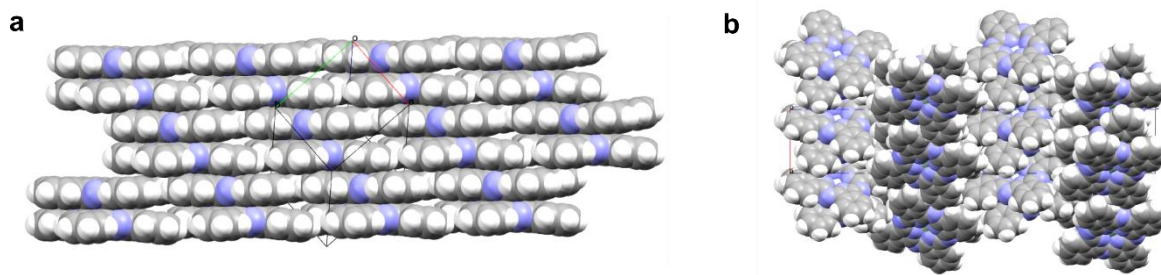


Figure 5. Space-filling model of the structure of the γ -phase, viewed along the $[\bar{1}12]$ (a) and the $[010]$ directions (b). Color code: Nd, light green; N, blue; C, grey; H, white.

The γ -phase of NdPc_2 was first identified in 1984 by comparing its powder pattern to that of the previously investigated SnPc_2 γ -phase.⁶³ The asymmetric unit in this phase is the full NdPc_2 molecule, showing barely curved Pc rings and the expected approximately square antiprismatic coordination mode, with Nd-N bond lengths in the range 2.455(3)-2.475(3) Å and a skew angle of $40.8^\circ(\pm 0.3)$. Parallel-displaced π - π interactions organize the NdPc_2 complexes in sheets along the (110) plane, with a bricklayer type stacking (slip angles $\varphi_1 = 47.3^\circ$, $\varphi_2 = 40.8^\circ$, twist angles $\psi_1 = \psi_2 = 0$). Nearest Nd-Nd distances within the sheets are 8.852(2) and 10.604(2) Å (**Figure 5a**). Successive sheets are rotated by 90° along the c axis, inducing alternating angles of $81.78(15)^\circ$ and $85.33(15)^\circ$ between the Pc-Pc axes of neighboring sheets (**Figure 5b**). Contact between the sheets corresponds to edge-on $\text{H}\cdots\text{H}$ contacts at a distance of 2.30-2.32 Å.

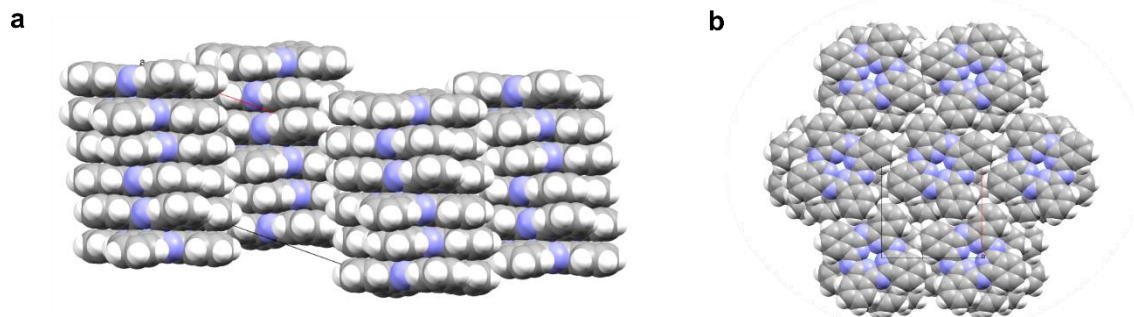


Figure 6. Space-filling model of the structure of the δ -phase, viewed along the $[010]$ (a) and the $[001]$ directions (b). Color code: Nd, light green; N, blue; C, grey; H, white.

The δ -phase, identified for the first time in 1986, was initially referred to as the β_2 polymorph, as it shares the $C2/c$ space group of the β -phase.¹⁸ The reported structure lacks H atoms and shows abnormal puckering in some of the benzene rings in the Pc ligands. X-ray diffraction studies conducted on crystals grown from solutions of air-oxidized NdPc_2^- allow us to now correct the record. In the δ -phase as in the β -phase, the asymmetric unit of the delta-phase is $\frac{1}{2}$ the molecule, with the full molecule generated by a 2-fold axis through the Nd^{3+} center parallel to the Pc ring. The resulting C_2 symmetry NdPc_2 complex displays Nd-N distances in the 2.468(3)-2.473(3) Å range and a skew angle of $42.7^\circ(\pm 0.5)$, higher than in phases α - γ but still lower than the 45° value of an ideal square antiprism. The NdPc_2 molecules are assembled via slipped stacking π - π interactions⁵² in vertical zig-zag columns (slip angle $\varphi = 67^\circ$), with shortest Nd-Nd distances of 7.0782(6) Å (**Figure 6a**). This particular columnar arrangement is correlated with the atypical curvature of the Pc rings, which take here a sigmoidal shape rather than the most commonly observed saucer shape. As in the β -phase, the Pc rings facing each other are aligned, as the twist angle $\psi = -42.7^\circ$ exactly compensates for the skew angle. Instead of the square lattice observed for the α - and β -phases, the stacks in the δ -phase are arranged in a hexagonal lattice (**Figure 6b**), similar to what has been observed for self-assembled monolayers of some substituted

phthalocyanine complexes.⁵⁴ The shortest distances between the interwoven neighboring stacks correspond to C \cdots H and H \cdots H distances of 2.782(4) Å and 2.31901(15) Å, respectively.

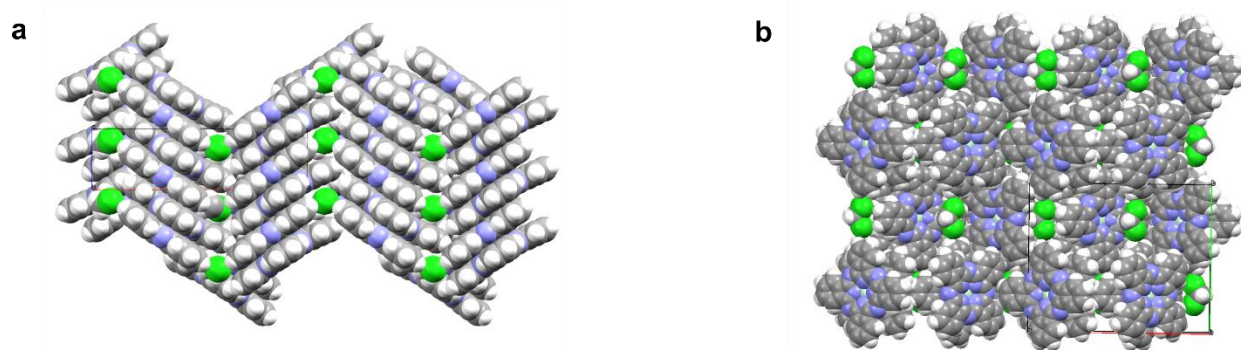


Figure 7. Space-filling model of the structure of the CH₂Cl₂ solvate phase, viewed along the [010] direction (a) and the [001] directions (b). Color code: Nd, light green; N, blue; Cl, bright green; C, grey; H, white.

The last polymorph is a CH₂Cl₂ solvate phase which has also been previously identified, though the space group was mis-assigned as P2₁2₁2₁ instead of Pnma.¹⁴ The asymmetric unit in this phase is again ½ the molecule, but this time the full molecule is generated by a mirror plane perpendicular to the Pc rings, imposing a skew angle of exactly 45°. Metal-ligand distances (2.4629(19)-2.477(3) Å) are identical with those of the other phases. Packing in this phase can be described by the formation of slipped columns of complexes via parallel π - π interactions (slip angle $\phi = 55.3^\circ$, twist angle $\psi = 0$, Nd-Nd distance 7.8897(4) Å), columns which are arranged in zig-zag chains (H \cdots H = 2.38428(9) Å) oriented perpendicular to the slip direction to form corrugated sheets (**Figure 7**). The dichloromethane molecules fill the corrugations. Finally, the planes of the Pc rings in alternate sheets are tilted by 70° to give a herringbone-type structure. Note however that contact between the sheets are limited to relatively short N \cdots H distances (2.64371(10) Å), and that no edge-to-face π - π interactions take place in the structure.

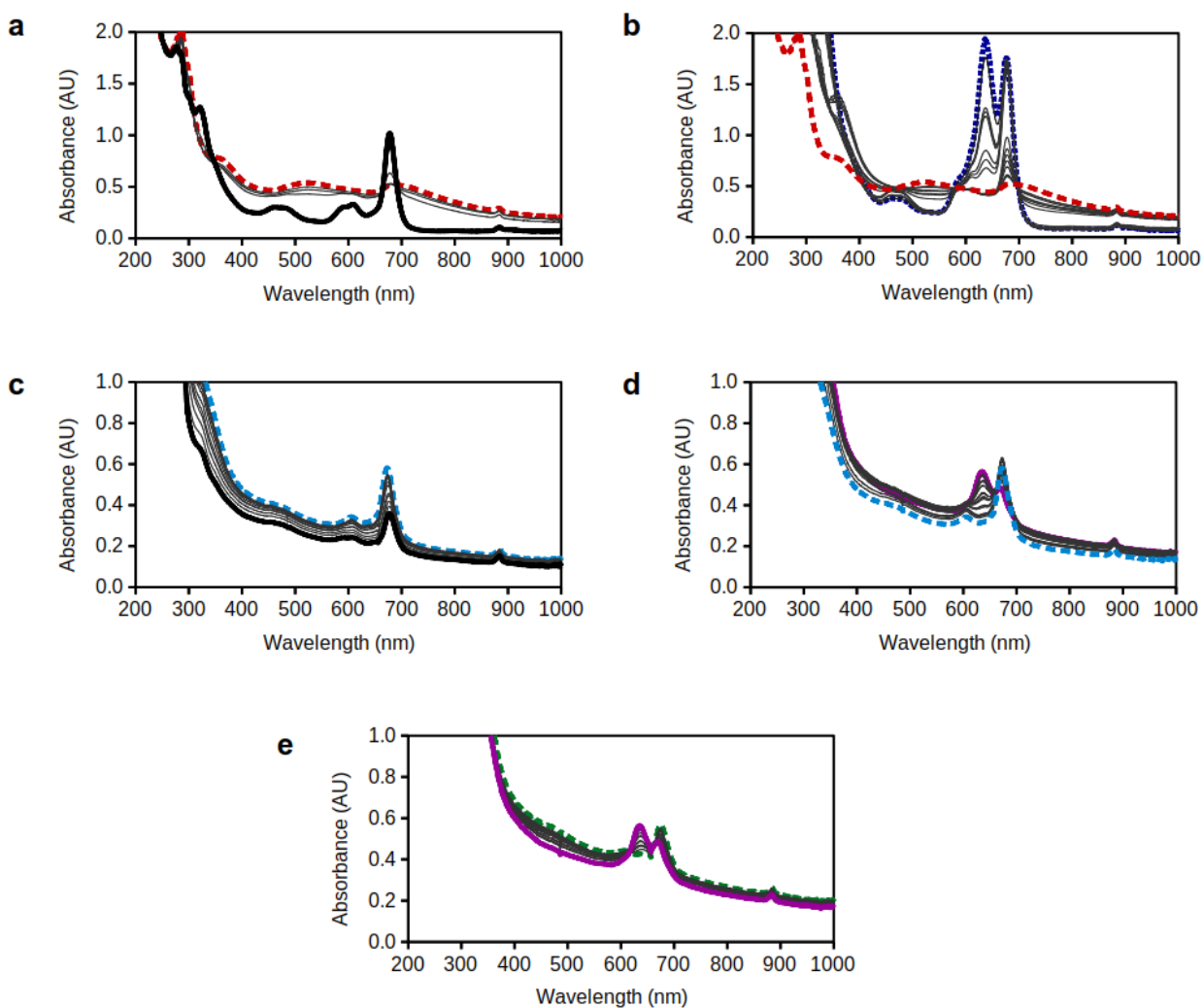


Figure 8. Spectrophotometric analysis of double-decker neodymium complexes. a) Addition of I_2 (0.05 M in CH_2Cl_2 , approx. 200 eqv.) to a solution of freshly dissolved α -phase crystals in CH_2Cl_2 oxidizes neutral $NdPc_2$ (approx. 5×10^{-7} M, solid black line) to $NdPc_2^+$ (dashed red line). b) Subsequent addition of NEt_3 (0.05 M in CH_2Cl_2 , approx. 3.5×10^3 eqv.) reduces $NdPc_2^+$ to $NdPc_2^-$ (dotted blue line). c) Addition of acetic acid (approx. 3.5×10^5 eqv.) to a solution of freshly dissolved γ -phase crystals in CH_2Cl_2 protonates $NdPc_2$ (solid black line) to $HNdPc_2^+$ (dashed blue line). d) Subsequent addition of DBU (approx. 8×10^5 eqv.) deprotonates and reduces $HNdPc_2^+$ to $NdPc_2^-$ (solid purple line). e) Subsequent addition of more acetic acid (approx. 1.6×10^6 eqv.) to the previous solution finally gives $HNdPc_2$ (dashed green line).

Table 2. A comparison of NdPc₂ species obtained by different titrations.

Species	NdPc ₂	NdPc ₂ ⁻	NdPc ₂ ⁺	HNdPc ₂ ⁺	HNdPc ₂
Q-Band Wavelength (nm)	678	638, 675	687	677	676

In previously published literature, the CH₂Cl₂ solvate phase was mistakenly described with the chemical composition NdPc₂H·CH₂Cl₂, with the additional proton delocalized over the eight chemically equivalent isoindole nitrogen atoms.¹⁴ Despite an X-ray photoelectron spectroscopy study, the authors were unable to prove the existence of the acidic H in the structure. In order to provide definitive references for the easy identification of NdPc₂, reduced protonated NdPc₂H and other related species including protonated HNdPc₂⁺, oxidized NdPc₂⁺ and reduced NdPc₂⁻, we recorded the UV-visible spectra of those species, obtained by chemical redox and acid-base conversion of high purity samples of NdPc₂ (Figure 8, Table 2).⁶⁴ Oxidation by I₂, a kinetically fast process, yields NdPc₂⁺, characterized by a red shift of the Q band, while NdPc₂⁻ is obtained by slow reduction by NEt₃ and shows a split Q band. Addition of a large excess of concentrated glacial acetic acid to a solution of NdPc₂ yields HNdPc₂⁺, which displays a very slightly red-shifted Q band and an additional peak at 605 nm. Deprotonation and simultaneous reduction of HNdPc₂⁺ by a large excess of concentrated DBU or NEt₃ yields NdPc₂⁻, which is protonated by a large excess of concentrated glacial acetic acid to form HNdPc₂. The latter complex has a very similar spectrum to that of neutral NdPc₂, explaining in part the confusion in the previous literature. We therefore recommend that any future speciation done on the basis of UV-Visible spectroscopy include careful titrations of the material.

CONCLUSIONS

Our investigation of NdPc₂ crystallization showed that it is possible to selectively grow crystals of four polymorphs by solvent slow evaporation, a convenient method affording larger amounts of material and better quality crystals than the previously reported electrochemical techniques. Good single crystals of these polymorphs allowed for a detailed structural analysis through single-crystal X-ray diffraction studies, including the correction of some mis-identifications in the previously published literature. The packing in all five known polymorphs is dominated by columnar stacking due to parallel π - π interactions, but some significant differences appear between phases in the arrangement of the columns, which is expected to have a significant impact on the conductivity properties of the material. The different polymorphs also exhibit a range of Nd-Nd distances (6.42-8.85 Å) and skew angles at the Nd center (39-45°) which will affect the magnetic properties. Additional studies are underway to fully explore the electronic and magnetic properties of these various polymorphs, and extend those results to other lanthanoid analogues.

ASSOCIATED CONTENT

Accession Codes CCDC 2016006-2016009 contain the supplementary crystallographic data for this paper. These data can be obtained free of charge via www.ccdc.cam.ac.uk/data_request/cif, or by emailing data_request@ccdc.cam.ac.uk, or by contacting The Cambridge Crystallographic Data Centre, 12 Union Road, Cambridge CB2 1EZ, UK; fax: +44 1223 336033.

AUTHOR INFORMATION

Corresponding Author

*Claire_Besson@gwu.edu.

Author Contributions

The manuscript was written through contributions of all authors. All authors have given approval to the final version of the manuscript.

ACKNOWLEDGMENT

The authors would like to thank the Cahill group of the George Washington University for the use of their single-crystal X-ray diffractometer. Maegan Dailey would especially like to thank J. August Ridenour of the Cahill group for always freely sharing his expertise.

REFERENCES

1. Kirin, I.S.; Moskalev, P.N.; Makashev, Y.A. Formation of Phthalocyanines of Rare-Earth Elements. *Zh Neorg Khim.* **1965**, *10*, 1951-1953.
2. Lenzoff, C.C.; Lever, A.B.P. *Phthalocyanines- Properties and Applications*; New York, 1989-1996
3. McKeown, N.B. *Phthalocyanine Materials- Synthesis, Structure and Function*; Cambridge University Press, New York, 1998.
4. Kadish, K.M.; Smith, K.M.; Guillard, R. *The Porphyrin Handbook Vol. 1-10*; Academic Press, San Diego, 2000.

5. Jiang, J.; Ng, D. A Decade Journey in the Chemistry of Sandwich-Type Tetrapyrrolo-Rare Earth Complexes. *Acc. Chem. Res.*, **2009**, *42*, 79-88.
6. Videlot, C.; Fichou, D.; Garnier, F. Photovoltaic Solar Cells Based on Rare-Earth Bisphthalocyanine Complexes. *Mol. Cryst. Liq. Cryst.*, **1998**, *322*, 319-328.
7. Chen Y.; Su, W.; Bai, M.; Jiang, J.; Li, X.; Liu, Y.; Wang, L.; Wang, S. High Performance Organic Field-Effect Transistors Based on Amphiphilic Tris(phthalocyaninato) Rare Earth Triple-Decker Complexes. *J. Am. Chem. Soc.*, **2005**, *127*, 15700-15701.
8. Ishikawa, N.; Sugita, M.; Wernsdorfer, W. Quantum Tunneling of Magnetization in Lanthanide Single-Molecule Magnets: Bis(phthalocyaninato)terbium and Bis(phthalocyaninato)dysprosium Anions. *Angew. Chem., Int. Ed.*, **2005**, *44*, 2931-2935.
9. Liu, Z.; Yasseri, A.A.; Lindsey, J.S.; Bocian, D.F. Molecular Memories that Survive Silicon Device Processing and Real-World Operation. *Science*, **2003**, *302*, 1543-1545.
10. De Cian, A.; Moussavi, M.; Fischer, J.; Weiss, R. Synthesis, Structure, and Spectroscopic and Magnetic Properties of Lutetium (III) Phthalocyanine Derivatives: $\text{LuPc}_2\cdot\text{CH}_2\text{Cl}_2$ and $[\text{LuPc}(\text{OAc})(\text{H}_2\text{O})_2]\text{H}_2\text{O}\cdot 2\text{CH}_3\text{OH}$. *Inorg. Chem.*, **1985**, *24*, 3162-3167.
11. Darovskikh, A.N.; Frank-Kamenetskaya, O.V.; Fundamenskii, V.S.; Golubev, A.M. The Crystal and Molecular Structure of Lutetium Diphthalocyanine (γ -Phase). *Kristallografiya*, **1986**, *31*, 279-283.
12. Darovsky, A.; Wu, L. Y.; Lee, P.; Sheu, H. S. Structure of Bis(phthalocyaninato)praseodymium (β 1 Phase). *Acta. Cryst.*, **1991**, *C47*, 1836-1838.

13. Darovsky, A.; Keserashvili, V.; Harlow, R.; Mutikainen, I. Structure of Oxidized Forms of Neodymium and Praseodymium (Bis)Phthalocyanines. *Acta Cryst.*, **1994**, *B50*, 582-588.
14. Kasuga, K.; Tsutsui, M.; Petterson, R.C.; Tatsumi, K.; Van Opdenbosch, N.; Pepe, G.; Meyer, E.F. Structure of Bis(phthalocyaninato)neodymium (III). *J. Am. Chem. Soc.*, **1980**, *102*, 4836-4838.
15. Sullivan, B.W.; Dominey, R.; Helms, J.; Schwartz, M.; ter Haar, L.; Hatfield, W. Preparation and Properties of Single Crystals of Hydrogen Bis(Phthalocyaninato) Neodymium(III). *Mol. Cryst. Liq. Cryst.*, **1985**, *120*, 433-436.
16. Darovskikh, A.N.; Tsytsenko, A.K.; Frank-Kamenetskaya, O.V.; Fundamenskii, V.S.; Moskalev, P.N. Polymorphism of Diphtalocyanine-Neodymium. Molecular and Crystal Structure of β Phase. *Sov. Phys. Crystallogr.*, **1984**, *24*, 273-276.
17. Darovskikh, A. Molecular and Crystal Structure of Tetragonal α -Phase of Neodymium Diphtalocyanine. *Krystallografiya*, **1986**, *31*, 901-905
18. Jullien, J.; Mossoyan-Déneux, M.; Pierrot, M.; Sorbier, J.; Fournel, A.; Benlian, D. On Two Conductive Species Derived from Bis(phthalocyaninato) Neodymium. *C. R. Acad. Sc. Paris.*, **1986**, *303*, 669-672.
19. Katoh, K.; Komeda, T.; Yamashita, M. Surface Morphologies, Electronic Structures, and Kondo Effect of Lanthanide(III)-Phthalocyanine Molecules on Au(111) by using STM, STS, and FET Properties for Next Generation Devices. *Dalton Trans.*, **2010**, *39*, 4708-4723.

20. Komijani, D.; Ghirri, A.; Bonizzoni, C.; Klyatskaya, S.; Moreno-Pineda, E.; Ruben, M.; Soncini, A.; Affronte, M.; Hill, S. Radical-Lanthanide Ferromagnetic Interaction in a TbIII Bis-Phthalocyaninato Complex. *Phys. Rev. Mater.*, **2018**, 2, 024405.
21. Ostendorp, G.; Homborg, H. Synthesis and Properties of the Diphthalocyaninates of Yttrium and Indium. *Z. Anorg. Allg. Chem.*, **1996**, 622, 1358-1364.
22. Katoh, K.; Yoshida, Y.; Yamashita, M.; Miyasaka, H.; Breedlove, B.K.; Kajiwarra, T.; Takaishi, S.; Ishikawa, N.; Isshiki, H.; Zhang, Y.; Komeda, T.; Yamagishi, M.; Takeya, J. Direct Observation of Lanthanide(III)-Phthalocyanine Molecules on Au(111) by Using Scanning Tunneling Microscopy and Scanning Tunneling Spectroscopy and Thin-Film Field-Effect Transistor Properties of Tb(III)- and Dy(III)- Phthalocyanine Molecules. *J. Am. Chem. Soc.*, **2009**, 131, 9967-9976.
23. Ostendorp, G.; Werner, J.; Homborg, H. Bis(phthalocyaninato)erbium (α_1 Phase). *Acta. Cryst.*, **1995**, C51, 1125-1128.
24. Haghighi, M.; Teske, C.; Homborg, H. Preparation, Properties and Crystal Structure of Bis(phthalocyaninato)cerium(IV). *Z. Anorg. Allg. Chem.*, **1992**, 608, 73-80.
25. Ostendorp, G.; Homborg, H. Synthesis, Properties and Crystal Structure of Di(phthalocyaninato)lanthanum(III), a Partially Oxidized Semiconductor. *Zeitschrift fuer Naturforschung, B: Chem. Sci.*, **1995**, 50, 1200-1206.
26. Gieren, A.; Hoppe, W. X-Ray Crystal Structure Analysis of Bisphthalocyaninatouranium (IV). *J. Chem. Soc. D*, **1971**, 413-415.

27. Darovskikh, A.N.; Frank-Kamenetskaya, O.V.; Fundamenskii, V.S.; Golynskaya, O.A. Refinement of the Molecular and Crystal Structure of Thorium Diphthalocyanine: Crystal Chemical Characteristics of a Monoclinic Modification of Diphthalocyanines of Actinides and Rare-Earth Elements. *Kristallografiya*, **1985**, *30*, 1085-1089.
28. Kobayashi, T. Crystal and Molecular Structures of Bisphthalocyaninat thorium (IV). *Bull. Inst. Chem. Res., Kyoto Univ.*, **1978**, *56*, 204-212.
29. Kirin, I.S.; Kolyadin, A.B.; Lychev, A.A. The X-Ray Diffraction Study of Thorium and Uranium Diphthalocyanine Complexes. *Russ. J. Struct. Chem.*, **1974**, *15*, 486-490.
30. Lux, F.; Beck, O.F.; Krauss, H.; Brown, D.; Tso, T.C. Spectroscopically Pure Bis(phthalocyaninato)protactinium(IV). *Z. Naturforsch., B: Chem. Sci.*, **1980**, *35B*, 564-567.
31. Moskalev, P. N.; Shapkin, G.N.; Darovskikh, A.N. Synthesis and Properties of Electrochemically Oxidized Diphthalocyanines of Rare Earth Elements and Americium. *Russ. J. Inorg. Chem.*, **1979**, *24*, 340-346.
32. Jancak, J.; Kubiak, R.; Jezierski, A. Synthesis, Crystal Structure, and Magnetic Properties of Indium(III) Diphthalocyanine. *Inorg. Chem.*, **1995**, *34*, 3505-3508.
33. Bennet, W.E.; Broberg, D.E.; Baenziger, N.C. Crystal Structure of Stannic Phthalocyanine, an Eight-Coordinated Tin Complex. *Inorg. Chem.*, **1973**, *12*, 930-936.
34. Janczak, J.; Kubiak, R. Crystal and Molecular Structure of Tin Bisphthalocyanine at 300 K (Monoclinic Form). *J. Alloy Compd.*, **1994**, *204*, 5-11.

35. Ostendorp, G.; Homborg, H. Synthesis and Properties of Diphthalocyaninates of Bismuth, $[\text{Bi}(\text{Pc})_2]^k$ ($k = 1-, 0, 1+$); Crystal Structure of Mixed-Valent $[\text{Bi}(\text{Pc})_2] \cdot \text{CH}_2\text{Cl}_2$. *Z. Anorg. Allg. Chem.*, **1996**, 622, 873-880.
36. Silver, J.; Lukes, P.; Howe, S.D.; Howlin, B. Synthesis, Structure, and Spectroscopic and Electrochromic Properties of Bis(phthalocyaninato)zirconium(IV). *J. Mater. Chem.*, **1991**, 1, 29-35.
37. Bian, Y.; Wang, D.; Wang, R.; Weng, L.; Dou, J.; Zhao, D.; Ng, D.; Jiang, J. Structural Studies of the Whole Series of Lanthanide Double-Decker Compounds with Mixed 2,3-Naphthalocyaninato and Octaethylporphyrinato Ligands. *New. J. Chem.*, **2003**, 27, 844-849.
38. Anyhan, M. M.; Singh, A.; Jeanneau, E.; Ahsen, V.; Zyss, J.; Ledoux-Rak, I.; Gürek, A.; Hirel, C.; Bretonnière, Y.; Andraud, C. ABAB Homoleptic Bis(phthalocyaninato)lanthanide(III) Complexes: Original Octupolar Design Leading to Giant Quadratic Hyperpolarizability. *Inorg. Chem.*, **2014**, 53, 4359-4370.
39. Jiang, J.; Bian, Y.; Furuya, F.; Liu, W.; Choi, M.; Kobayashi, N.; Li, H.; Yang, Q.; Mak, T.; Ng, D. Synthesis, Structure, Spectroscopic Properties, and Electrochemistry of Rare Earth Sandwich Compounds with Mixed 2,3-Naphthalocyaninato and Octaethylporphyrinato Ligands. *Chem. Eur. J.*, **2001**, 7, 5059-5069.
40. Fahrenndorf, S.; Matthes, F.; Bürgler, D. E.; Schneider, C. M.; Atodiresei, N.; Caciuc, V.; Blügel, S.; Besson, C.; Kögerler, P. Structural Integrity of Single Bis(Phthalocyaninato)-Neodymium(III) Molecules on Metal Surfaces with Different Reactivity. *Spin*, **2014**, 4, 11440007-11440018.

41. SAINT; Bruker AXS. Inc.: Madison Wisconsin, USA, 2007.
42. APEX II; Bruker AXS Inc.: Madison, WI, 2008.
43. Krause, L.; Herbst-Irmer, R.; Sheldrick, G.M.; Stalke, D. Comparison of Silver and Molybdenum Microfocus X-Ray Sources for Single-Crystal Structure Determination. *J. Appl. Crystallogr.*, **2015**, *48*, 3-10.
44. Altomare, A.; Cascarano, G.; Giacovazzo, C.; Guagliardi, A.; Burla, M. C.; Polidori, G.; Camalli, M. SIR92 – A Program for Automatic Solution of Crystal Structures by Direct Methods. *J. Appl. Crystallogr.*, **1994**, *27*, 435.
45. Sheldrick, G. M. Crystal Structure Refinement with SHELXL. *Acta Crystallogr., Sect. C: Struct. Chem.*, **2015**, *71*, 3-8.
46. Farrugia, L. J. WinGX Suite for Small-Molecule Single-Crystal Crystallography. *J. Appl. Crystallogr.*, **2012**, *45*, 849-854.
47. Hübschle, C.B.; Sheldrick, G.M.; Dittrich, B. ShelXle: a QT Graphical User Interface for SHELXL. *J. Appl. Cryst.*, **44**, 2011, 1281-1284.
48. Spek, A.L. Single-crystal Structure Validation with the Program PLATON. *J. Appl. Crystallogr.*, **2003**, *36*, 7-13.
49. Macrae, C. F.; Edgington, P. R.; McCabe, P.; Pidcock, E.; Shields, G. P.; Taylor, R.; Towler, M.; van de Streek, J. Mercury: Visualization and Analysis of Crystal Structures. *J. Appl. Crystallogr.*, **2006**, *39*, 453-457.
50. McKeown, N.B. Phthalocyanines and Related Compounds. *Sci. Synth.*, **2004**, *17*, 1237.

51. Ostendorp, G.; Homborg, H. Synthesis and Spectroscopical Properties of the Mixed-Valent Di(phthalocyaninato)lanthanides(III). *Z. Anorg. Allg. Chem.*, **622**, 1996, 1222-1230.
52. Yao, Z.; Wang, J.; Pei, J. Control of π - π Stacking via Crystal Engineering in Organic Conjugated Small Molecule Crystals. *Cryst. Growth Des.*, **18**, 2018, 7-15.
53. Komeda, T.; Isshiki, H.; Liu, J.; Katoh, K.; Yamashita, M. Variation of Kondo-Temperature Induced by Molecule-Substrate Decoupling in Film Formation of Bis(phthalocyaninato)terbium(III) Molecules on Au (III). *ACS Nano*, **8**, 2014, 4866-4875.
54. Ara, F.; Qi, Z.; Hou, J.; Komeda, T.; Katoh, K.; Yamashita, M. A Scanning Tunneling Microscopy Study of the Electronic and Spin States of Bis(phthalocyaninato)terbium(III) (TbPc₂) Molecules on Ag(III). *Dalton Trans.*, **45**, 2016, 16644-16652.
55. Serrano, G.; Wiespointner-Baumgarthuber, S.; Tebi, S.; Klyatskaya, S.; Ruben, M.; Koch, R.; Müllegger, S. Bilayer of Terbium Double-Decker Single-Molecule Magnets. *J. Phys. Chem. C.*, **2016**, *120*, 13581-13586.
56. Gottfried, J. Surface Chemistry of Porphyrins and Phthalocyanines. *Surf. Sci. Rep.*, **70**, 2015, 259-379.
57. Komeda, T.; Isshiki, H.; Liu, J.; Zhang, Y.; Lorente, N.; Katoh, K.; Breedlove, B.; Yamashita, M. Observation and Electric Current Control of a Local Spin in a Single-Molecule Magnet. *Nature Comm.*, **217**, 2011, 1-7.
58. Gopakumar, T.G.; Brumme, T.; Kröger, J.; Toher, C.; Cuniberti, G.; Berndt, R. Coverage-Driven Electronic Decoupling of Fe-Phthalocyanine from a Ag(111) Substrate. *J. Phys. Chem. C.*, **115**, 2011, 12173-12179.

59. Zhang, Y.; Isshiki, H.; Katoh, K.; Yoshia, Y.; Yamashita, M.; Miyasaka, H.; Breedlove, B.; Kajiwar, T.; Takaishi, S.; Komeda, T. Low-Temperature Scanning Tunneling Microscopy Investigation of Bis(phthalocyaninato)yttrium Growth on Au(111): From Individual Molecules to Two-Dimensional Domains. *J. Phys. Chem. C.*, **113**, 2009, 9826-9830.
60. Fu, Y.; Schwöbel, J.; Hla, S.; Dilullo, A.; Hoffmann, G.; Klyatskaya, S.; Ruben, M.; Wiesendanger, R. Reversible Chiral Switching of Bis(phthalocyaninato) Terbium(III) on a Metal Surface. *Nano Lett.*, **12**, 2012, 3931-3935.
61. Deng, Z.; Rauschenbach, S.; Stepanow, S.; Klyatskaya, S.; Ruben, M.; Kern, K. Self-Assembly of Bis(phthalocyaninato)terbium on Metal Surfaces. *Phys. Scr.*, **90**, 2015, 1-9.
62. Inose, T.; Tanaka, D.; Tanaka, H.; Ivasenk, O.; Nagata, T.; Ohta, Y.; De Feyter, S.; Ishikawa, N.; Ogawa, T. Switching of Single-Molecule Magnetic Properties of Tb^{III}-Porphyrin Double-Decker Complexes and Observation of Their Supramolecular Structures on a Carbon Surface. *Chem. Eur. J.*, **20**, 2014, 11362-11369.
63. Mossoyan-Deneux, M.; Benlian, D.; Baldy, A.; Pierrot, M. Crystal Structures of Tetragonal NdPc₂O and NdPc₂Cl_xO_{1-x} Obtained from NdPc₂H by Anodic Crystal Growth. *Mol. Cryst. Liq. Cryst. Inc. Nonlin. Opt.*, **1988**, 156, 247-256.
64. The spectra of some of those species reported previously occasionally suffer from miss-assignment of protonation or redox states and/or aggregation issues leading to broadened spectra. Molar absorption coefficients, when present, vary greatly from reference to reference, suggesting widespread contamination of the samples.